Resonant mode characterisation of a cylindrical Helmholtz cavity excited by a shear layer

Gareth J. Bennett[a] and David B. Stephens[b]
Department of Mechanical and Manufacturing Engineering, School of Engineering, Trinity College Dublin, the University of Dublin, Dublin D02 PN40, Ireland

Francisco Rodriguez Verdugo[c]
Dipartimento di Ingegneria Meccanica Industriale, Universita degli Studi Roma Tre, Rome, Italy

(Received 29 August 2016; revised 23 November 2016; accepted 8 December 2016; published online 3 January 2017)

This paper investigates the interaction between the shear-layer over a circular cavity with a relatively small opening and the flow-excited acoustic response of the volume within to shear-layer instability modes. Within the fluid-resonant category of cavity oscillation, most research has been conducted on rectangular geometries: generally restricted to longitudinal standing waves, or when cylindrical: to Helmholtz resonance. In practical situations, however, where the cavity is subject to a range of flow speeds, many different resonant mode types may be excited. The current work presents a cylindrical cavity design where Helmholtz oscillation, longitudinal resonance, and azimuthal acoustic modes may all be excited upon varying the flow speed. Experiments performed show how lock-on between each of the three fluid-resonances and shear-layer instability modes can be generated. A circumferential array of microphones flush-mounted with the internal surface of the cavity wall was used to decompose the acoustic pressure field into acoustic modes and has verified the excitation of higher order azimuthal modes by the shear-layer. For azimuthal modes especially, the location of the cavity opening affects the pressure response. A numerical solution is validated and provides additional insight and will be applied to more complex aeronautical and automotive geometries in the future. © *2017 Acoustical Society of America*.
[http://dx.doi.org/10.1121/1.4973212]

[DDE] Pages: 7–18

I. INTRODUCTION

Shear layer driven cavity flows can exhibit several types of features generally described as resonance. The review paper of Rockwell and Naudascher[1] categorized self-sustaining oscillations into three groups: fluid-dynamic, fluid-resonant, and fluid-elastic. Of these, self-sustaining cavity oscillations which are strongly coupled with resonant waves within the shear layer may be classified as fluid-resonant oscillations. Oscillations of this class occur at sufficiently high frequencies such that the corresponding acoustic wavelength is of the same order of magnitude, or smaller, than the cavity characteristic length-considered here to be the height of the cylindrical cavity, H. For ideal organ pipe conditions, these oscillations are predicted to have an acoustic wavelength of $\lambda \leq 2H$ for a closed cavity end condition of diameter D. The exact frequency at which these longitudinal modes (standing waves along the height of the cavity) occur for shear layer driven oscillations is complicated by the very presence of the shear layer. Within the fluid-dynamic category, a highly cited work is for high Mach number ($M > 0.5$) flow over a shallow cavity known as a Rossiter cavity.[2] In this system, the feedback mechanism is an upstream-traveling acoustic wave which has been generated by turbulent structures impacting the downstream edge of the cavity. These acoustic waves have a wavelength close to the cavity opening dimension, or length, L. Resonance occurs if this acoustic frequency can excite the shear layer oscillation. The fluid-elastic category occurs when one or more wall of the cavity undergoes a displacement that exerts a feedback control on the shear layer perturbation. For cavities with rigid boundaries, the fluid-resonant category may contribute significantly to unwanted noise: from aircraft landing gear wheel bays, for example, or to undesirable pressure pulsations such as may be experienced in vehicles with open windows. A study by Langtry and Spalart[3] used computational methods to predict the unsteady pressure inside a landing gear wheel well on a commercial aircraft geometry. Balasubramanian *et al.*[4] and Ricot *et al.*[5] have considered "sunroof buffeting" on a simplified vehicle geometry. Tonon *et al.*[6] have studied a series of side branch resonators as a model for flow in a corrugated pipe. Height modes were also studied by Yang *et al.*[7] who specifically analyzed the effect of the stream wise dimension of the cavity and a coaxial side branch configuration was studied by Oshkai and Yan.[8]

Panton and Miller[9] conducted seminal work on Helmholtz resonance which has been revisited by Kook and Mongeau[10] and Ma *et al.*[11] who have all more recently studied Helmholtz resonators and accurately predicted the magnitude of the interior cavity pressure, when adequate information about the shear layer is available. Elder[12] experimentally investigated a

[a]Electronic mail: gareth.bennett@tcd.ie
[b]Current address: NASA Glenn Research Center, Cleveland, OH, 44070, USA.
[c]Current address: Loccioni Via Fiume 16, 60030 Angeli di Rosora, Ancona, Italy.

deep cylindrical cavity with a rectangular opening. He characterized the shear layer with a hot wire probe sampled simultaneously with a microphone at the bottom wall of the cavity: after phase-averaging the velocity, shear layer profiles at different phases during an acoustic cycle were presented. Diametral acoustic modes have been explored for an axisymmetric shallow cavity configuration in a work by Awny and Ziada,[13] and the work of Oshkai *et al.*[14] employs PIV techniques to gain further insight into the study of shear layer flows.

In an attempt to suppress cavity noise, a number of different methods have been investigated: active fluid-injection methods such as micro-jets and leading edge blowing, plasma actuators, the installation of a cross-flow rod at the cavity leading edge, and the installation of Helmholtz resonators within the cavity environment.[15] There have been a number of excellent reviews of cavity noise dynamics and suppression published.[16,17]

To date, within the fluid-resonant category, almost no consideration has been given to higher order acoustic modes which might resonate in cavities, whether cylindrical or polyhedral in shape. An exception to this is a recent study by Marsden *et al.*,[18] which states that cylindrical burst-disk cavities and vent holes located under wings have been subject to little investigation, despite being clearly identifiable in flyover measurements. In this paper, we are particularly interested in exploring the test case where a number of different types of resonant behavior can be excited depending on flow speed or orifice geometry. In practical cases, such as for aircraft take-off and landing where the flow speed varies, it is important to be able to predict these modes so that mitigation measures can be implemented for all modes excited. Recent research published from EU Green Regional Aircraft Clean Sky projects[19–21] have demonstrated success in the reduction of nose and main landing gear noise on full and half scale models with the use of low noise technologies. However, the wheel bays continue to be a significant noise source, and for approach and landing, velocities were found to radiate tones at both the Helmholtz resonance frequency of the nose landing gear wheel bay[22] and also at frequencies which were higher than the first, and most typically studied, depth mode for both the nose and main landing gear.[23,24] The work in the current paper seeks to investigate, in addition to the most typically examined longitudinal mode, both the Helmholtz resonance and the higher order resonant modes of cavities: modes which are often neglected. Unexpected combination modes are also predicted and measured. The study attempts to stress the importance of these other modes to designers who may typically only examine plane wave depth modes and integer multiples thereof.

II. ACOUSTIC PRESSURE FIELD IN A CYLINDRICAL DUCT

The cavities to be considered in this experimental work are cylindrical with large H/D but small L/D ratios. As a consequence of this, we can approximate the cavity to be a closed-ended cylindrical duct such as depicted in Fig. 1. The most common situation to be found in the literature is for a plane travelling acoustic wave which reflects from the end to form a standing wave. In cylindrical ducts, plane waves, only, can propagate below a characteristic frequency which is a function of the duct diameter. In this paper, higher order acoustic modes which are excited above this frequency are also considered.

A. Mode propagation in hard walled cylindrical ducts

For acoustic propagation in hard walled cylindrical ducts with superimposed constant mean flow, the solution to

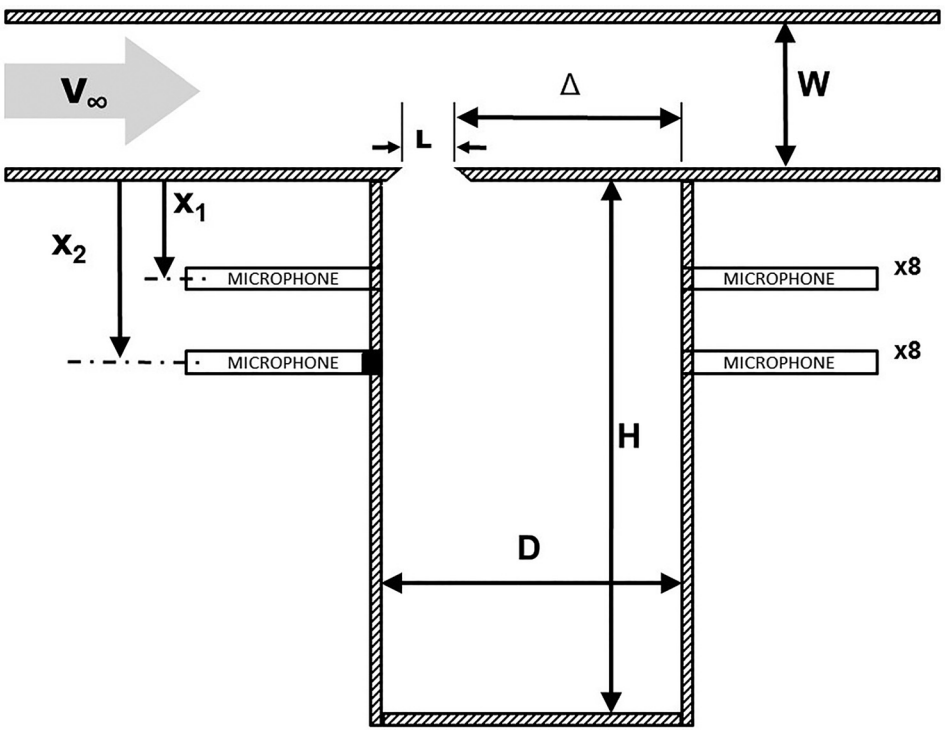

FIG. 1. Schematic of the square wind tunnel test section and the cylindrical cavity. The cylinder is instrumented with two rings of eight microphones flush mounted with the internal surface and distributed equally around the circumference. Section taken through the central plane. Not to scale.

the convective wave equation may be expressed, in cylindrical coordinates, as a linear superposition of modal terms

$$\hat{p}(x,r,\theta,\omega) = \sum_{m=-\infty}^{+\infty} A_m(x,r,\omega)e^{jm\theta}, \tag{1}$$

where

$$A_m(x,r,\omega) = \sum_{n=0}^{\infty}[A^{+}_{m,n}e^{-jk^{+}_{m,n}x} + A^{-}_{m,n}e^{+jk^{-}_{m,n}x}]f_{m,n}(k_{r,m,n}(r/R)). \tag{2}$$

The complex pressure $\hat{p}(x,r,\omega,\theta)$ is a solution to the Helmholtz equation and $A_m(x, r, \omega)$ is the complex modal magnitude of the azimuthal modes of order m which may be further decomposed into a series of radial modes of order n. The modal shape eigenvector $f_{m,n}(k_{r,m,n}(r/R))$ is a suitably normalised form of the Bessel function of the first kind which describes the radial acoustic pressure distribution dependent on the duct cross-sectional geometry. $k_{r,m,n}$ is the transverse eigenvalue of the (m, n)th mode and is also called the transverse, combined radial-circumferential or simply the radial wavenumber k_r.

Once these higher order acoustic modes, $A^{\pm}_{m,n}$, are "cut-on," they may propagate energy along the duct in much more complicated pressure patterns than that of the plane wave mode which varies only in the longitudinal direction. In contrast, these higher order modes may vary in both the azimuthal and radial directions of order m and n, respectively. This occurs when these modes, of axial wavenumber $k^{\pm}_{m,n}$, are excited above a cut-on frequency which depends on the mode eigenvalue and the duct radius. Modes excited below their cut-on frequency are evanescent and decay exponentially with distance along the duct. The dimensionless number which expresses the cut-on point of each independent higher order mode is the Helmholtz number (He) or term $kR = (2\pi fR)/c$. When more than one mode has cut-on, these modes are superimposed upon the plane wave mode and can co-exist with each other over a range of frequencies. The modes may propagate in either the positive or negative direction as indicated by the $\pm$ superscripts. Azimuthal modes may also rotate in the clockwise or counterclockwise direction as they propagate along a duct.

Modal decomposition is an advanced experimental technique which can provide detailed information of the modal content of sound propagating in ducts. In this work, the higher order modal content of a cylindrical cavity is examined analytically, numerically, and its response to excitation by a fluctuating shear layer is measured with a flush mounted array of microphones. These measurements are used to perform an acoustic modal decomposition of the cavity pressure field and to calculate directly the modal content of the duct in response to the shear layer excitation as a function of frequency. The results are compared to the analytical and numerical predictions.

B. Applied modal decomposition method

The modal decomposition technique used in this work is that of Bennett,[25] which is based closely on the methods of Åbom[26] and Yardley.[27] The method employs an array of microphones mounted flush to the inner duct wall surface. The sensors in this array are spaced equally both azimuthally and axially. The characteristics and advantages of this technique for duct/aeroengine noise are (1) both incident and reflected modes can be identified, (2) a mean flow can be accommodated when present, (3) a frequency response function technique may be employed, (4) radial, as well as azimuthal, modes can be identified, (5) duct-wall flush-mounted microphones only are used for the decomposition, (6) the decomposition is performed for all frequencies and not only at specific tones such as rotor blade-pass frequency (BPF) and harmonics thereof when present, (7) data are acquired at all measurement locations simultaneously allowing for coherence analysis.

From the formulation of the acoustic pressure in a hard-walled duct given by Eqs. (1) and (2), this modal decomposition technique is undertaken in two stages. More complete detail on both stages can be found in the technical report by Åbom.[28] In the first stage, an azimuthal decomposition is carried out using microphones located circumferentially around the duct as follows:

$$\frac{\hat{p}_{l,k}}{\hat{p}_{ref}} = \sum_{m=1-M}^{M-1} h_{m,k}e^{[jm\theta_l]}, \quad \text{where} \quad \begin{aligned} &l = 0, 1, \ldots, 2M-2, \\ &k = 0, 1 \ldots, 2N-1, \\ &\theta_l = \frac{2\pi l}{2M-1}, \end{aligned} \tag{3}$$

where M and N are the number of azimuthal and radial modes cut-on at the frequency of interest. Referring to Fig. 2, l and k are shown to be the circumferential and axial indices of a specific microphone in the array. Equation (3) is a discrete form of Eq. (1), where both sides of the equation have also been divided by the complex pressure from a reference microphone. This transfer function form of the equation is useful

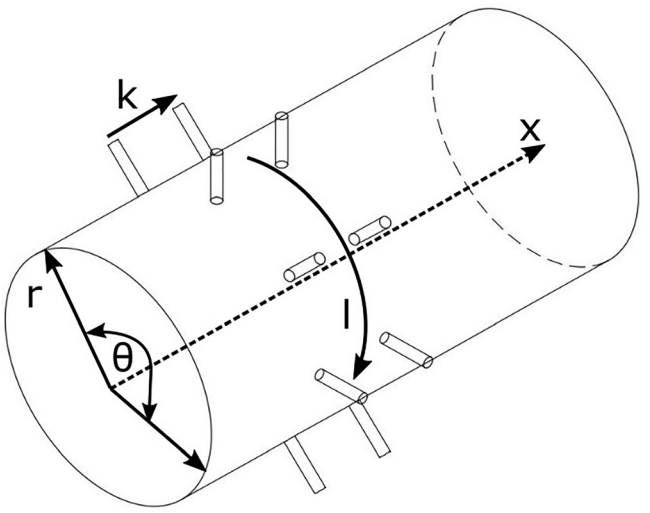

FIG. 2. Polar coordinate system for the cylindrical duct (x, r, θ). Microphones are distributed equi-spaced in the azimuthal direction and are indexed with $l = 0, 1, \ldots, 2M-2$. Additional rings of microphones in the x-direction are indexed with $k = 0, 1, \ldots, 2N-1$.

as the phase of the modes can be referenced to a single location and the approach also allows for microphone calibration. Using this method, an azimuthal modal analysis may be performed at a specific axial location in a duct using microphones flush-mounted to the duct inner wall.

This azimuthal modal analysis may be repeated at several axial locations in order to further decompose these modes into both the radial modes and their incident and reflected components

$$h_{m,k} = \sum_{n=0}^{N-1} [A^{+}_{m,n} e^{-jk^{+}_{m,n}x} + A^{-}_{m,n} e^{+jk^{-}_{m,n}x}] f_{m,n}(r). \quad (4)$$

Using a process of matrix pseudo-inversion, a least-squares solution can be found for the above equation to estimate the complex radial modal amplitudes. Typically, the system is over-determined using more than the minimum required number of microphones to stabilise the pseudo-inversion process and reduce the possibility of singularities appearing at circumferential and axial drop-out frequencies. Poor matrix conditioning can be mitigated using a system of matrix regularisation to increase the robustness of the pseudo-inversion step (particularly close to modal cut-on), however, such methods introduce additional uncertainty in the modal estimation.[29]

The first part of the technique (the azimuthal modal analysis) requires a minimum of two measurements per azimuthal wavelength ($2\pi/m$), in accordance with the Nyquist sampling criterion. At least $2M$ sensors are therefore required to be located azimuthally, where M is the highest azimuthal mode order cut-on in the frequency range under investigation. This places an upper frequency limit at which this technique can be applied for a given number of acoustic sensors. Holste and Neise[30] make similar conclusions, and also state that aliasing is possible when an insufficient number of sensors are installed per mode cut-on. An example of the full expansion of this modal decomposition procedure can be found in Chap. 7 of Ref. 31 for a specific experimental set-up.

III. EXPERIMENTAL RIG DESIGN

A cavity resonance experiment that incorporates each of the three feedback mechanisms has been designed and constructed. As the rig was to be built using a small, low speed wind tunnel, preliminary analysis was required in order to optimally design the cavity given the imposed limitations. In each of the three fluid-resonant oscillations considered in this paper, viz., Helmholtz resonance, longitudinal resonance, and azimuthal resonance, the acoustic excitation is assumed to be due to instability in the shear layer of flow over the cavity opening. The shear layer excitation frequency can be estimated using the empirical relationship suggested by Rossiter.[2] Given the low Mach number under consideration in the current paper ($M < 0.15$), the upstream-propagating fluid-dynamic acoustic feedback mechanism usually associated with Rossiter is not expected to occur in the present experiment, because the acoustic frequency corresponding to the cavity opening length would be in the order of 8 kHz, far higher than any expected shear layer oscillation frequency for the flow speeds explored here. Rossiter's equation for the shear layer excitation frequency, however, has been used by many authors to accurately model other feedback mechanisms.[11,32] This equation is given as

$$St \equiv \frac{fL}{U} \approx \frac{n-\alpha}{M+\frac{1}{\kappa}}, \quad (5)$$

where α describes the phase delay between the hydrodynamic forcing and the acoustic feedback and κ is the convection velocity of the shear layer normalized by the free stream velocity and $n = 1, 2, 3,\ldots$ is the order of the shear layer mode. For the low subsonic speeds considered here, $\alpha = 0$ was found to be appropriate, and has been used by other authors,[11,33,34] who argued that there is no need to consider a phase delay when the convection speed is much less than the speed of sound. The typical value of $\kappa = 0.5$ is the average of the free stream speed and the flow in the cavity, and does not include effects of the boundary layer which acts to retard the apparent free stream velocity. Over the years, Eq. (5) has been subject to small changes introduced after analytical developments: see, for instance, Heller and Bliss[35] and Howe.[36]

As can be seen in Eq. (5), decreasing the characteristic length of the cavity opening, L, increases the excitation frequency for a given flow speed. Similarly, from knowledge of duct acoustics and of the Helmholtz number, increasing the cavity diameter will result in lower cut-on frequencies for the higher order modes. Thus, for the low tunnel speeds available, a large diameter and short streamwise length orifice was required to achieve the test objectives allowing excitation of the three different fluid-resonance categories considered. Schematics of the cavity and opening can be seen in Figs. 1 and 3. The large diameter of the cylinder was selected in order to reduce the frequency at which higher-order azimuthal acoustic modes are cut-on. The first azimuthal mode should cut-on at approximately 846 Hz for this diameter assuming closed/closed end conditions. Initially, a 40 mm square opening with sharp edges connected the cavity to the wind tunnel, however, openings of different length and location relative to the cavity centerline were also tested and are discussed in Sec. IV D.

A. Numerical analysis—Wave expansion method (WEM)

In order to verify the cavity design prior to construction, initially an examination of the analytical solution of the pressure field in a cylindrical duct was performed. The boundary conditions chosen were for a hard walled closed-closed cylinder. Given the small size of the opening and the large H/D ratio, it was thought that this approach would provide a reasonably representative response. However, the effect of the opening, especially at higher frequencies could not predicted and so, in addition, a series of numerical simulations were performed on a meshed domain of equal dimensions to the air volume of the proposed design. As the authors are also interested in investigating the excitation of higher-order

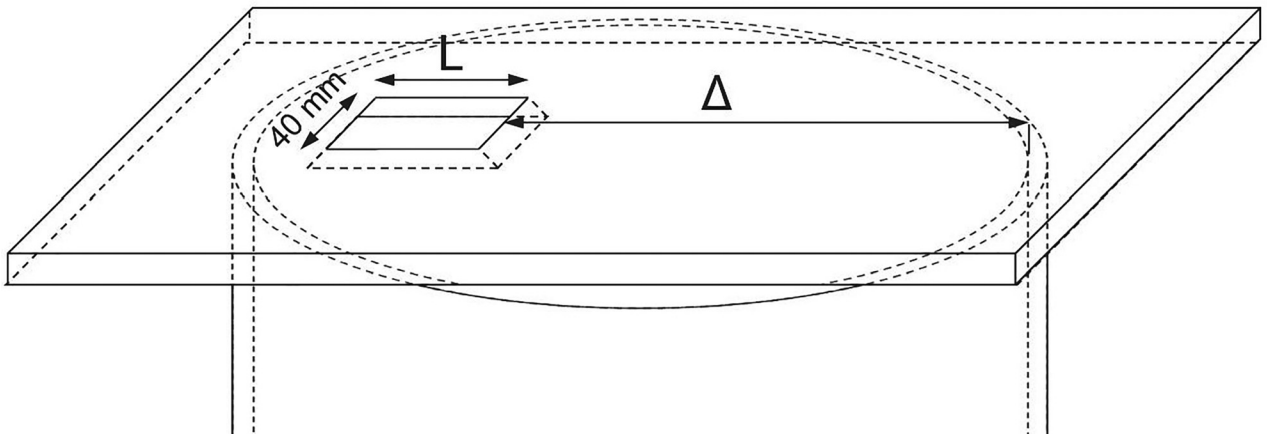

FIG. 3. Schematic of the cavity opening. Openings of different length and location relative to the cavity centerline were tested and are discussed in Sec. IV D.

acoustic modes in more complex volumes such as the interior of cars and aircraft landing-gear bays for which there are no analytical solutions, this numerical development was conducted as much as a validation exercise in the applicability of the method itself as it was to provide design and performance insight into this particular geometry. A highly efficient finite difference method originally introduced by Caruthers *et al.*[37] was used for the analysis. The approach uses wave functions which are exact solutions of the governing differential equation. The wave expansion method (WEM) code used for this study was further developed by Ruiz and Rice[38] and Barrera Rolla and Rice[39] to investigate sound propagation in quiescent media and has been examined by Bennett *et al.*[40] for its applicability in ducts. In order to simulate an oscillation in the shear layer, a numerical monopole volume source was located at the orifice opening mid-point. The complex pressure is solved in the domain as a function of source frequency and the amplitude can be plotted on the mesh to give an indication of the pressure field in the cavity/wind tunnel rig set-up.

1. Implementation and analysis

A three-dimensional unstructured mesh encompassing the wind tunnel test section and the cavity was generated with the commercial software Gambit, resulting in approximately 240 000 tetrahedral elements (Fig. 4). Based on an initial estimate of frequencies and on available material sizes for construction of the model, the dimensions of the cylinder were chosen to be $D = 238$ mm and $H = 493$ mm. As the largest cell in the mesh measures 0.0185 m, the highest frequency of interest (1838 Hz) is therefore resolved with at a minimum of ten grid points per wavelength. In the opening region, the mesh was refined in order to have at least the same resolution as PIV measurements which were conducted in accompanying studies of this system.[41,42]

As stated, the system was excited by a monopole source located in the center of the opening. A preliminary parametric study showed that the location of the monopole source does not have any significant influence on the shape and the frequency of the modes. The inlet and the outlet of the square test section were modelled with radiation boundary conditions.

The response of the system as a function of frequency was determined by running the code in a loop over 1000 different frequencies in the range [46–1838 Hz] or up to approximately $\mathrm{He} = 4$. In this frequency range, 17 different acoustic modes were found. By way of illustration, two of these are presented in Fig. 5.

As discussed, the common nomenclature in cylindrical duct acoustics is for the subscript m to indicate the azimuthal order and the subscript n to indicate the radial order. Of additional interest in this current study is the measurement of the end reflection from the cavity which causes the longitudinal standing wave and its superposition on the azimuthal/radial modes, thus the third subscript q is used to indicate the depth mode order. For example, $A_{m,n,q} = A_{0,0,1}$ is the first half wavelength depth/longitudinal mode and is also named here as the H1 mode given that H is the depth of the cavity as per Fig. 1. The first azimuthal mode is termed AZ1 and in Fig. 5 the combination mode AZ1H2 $A_{m,n,q} = A_{1,0,2}$ is illustrated. No radial modes were excited in the range of wind tunnel speeds tested in the subsequent experimental campaign and therefore results presented here will be for $n = 0$, i.e., $A_{m,0,q}$.

The mode shapes calculated by the WEM analysis seem similar to the shapes of the analytical modes that would be calculated inside a completely closed cylinder. In order to

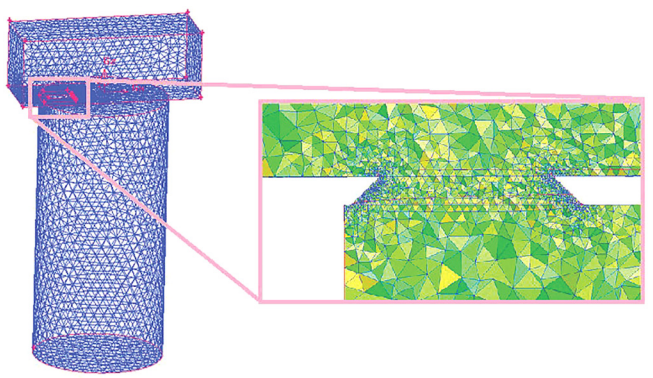

FIG. 4. (Color online) Computational domain meshed for the WEM calculation. Detail of the mesh in the opening area. Section taken through the central plane.

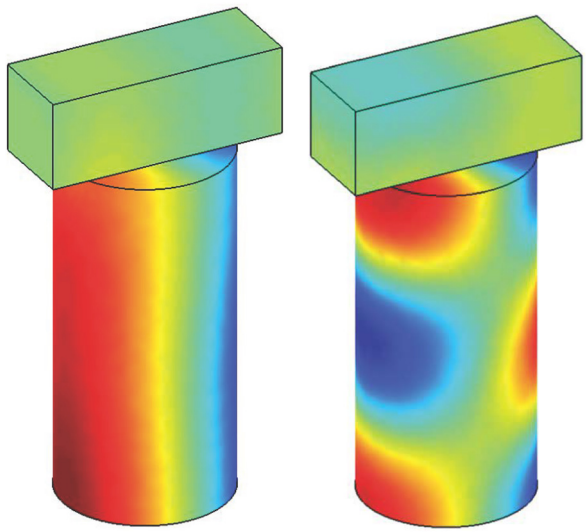

(a) AZ1 (b) AZ1H2

FIG. 5. (Color online) Numerical WEM results: normalized real pressure response of the cavity to monopole excitation at orifice opening of cavity to wind tunnel test section. Two acoustic resonances are shown: (a) first azimuthal mode AZ1 (He = 1.85, $A_{m,n,q} = A_{1,0,0}$); (b) second azimuthal-longitudinal combination mode AZ1H2 (He = 2.42 $A_{m,n,q} = A_{1,0,2}$).

appreciate the differences between these two cases, the real part of the complex pressure is analysed along the middle plane of the cavity (Fig. 6). Unsurprisingly, the opening not only modifies the pressure in the orifice vicinity, as shown by the first longitudinal mode, but in some cases, the pressure pattern changes everywhere inside the cavity: the third longitudinal mode clearly illustrates this shape distortion.

The frequencies of the first 7 WEM modes (up to He = 3) are given in Table I. Differences can be noticed when they are compared with the analytical case. These differences are generated by the distortion of the pressure pattern. The pressure reduces in the test section which induces a pressure adaptation in proximity to the orifice. These effects are more significant for some modes, such as the H1 and AZ1H1 mode (15 Hz difference) compared to others, such as the H3 mode which has only a 5 Hz difference between the WEM and analytical solution. The effects of the opening are similar to a reduction of the cavity depth. Consequently, the frequencies of the modes increase. An illustration of this is given by the mode AZ1H1 [Fig. 6(b)]: there is a clear virtual reduction of the cavity depth, compared to the closed case, as measured at the microphone location illustrated by the black square.

Based on the results of this analysis, it was confirmed that this cavity geometry would allow all three fluid-resonant category configurations to be excited by a cavity orifice length L of approximately 40 mm/45 mm in the flow range of the wind tunnel available for the tests.

B. Test set-up

A draw-down wind tunnel with an elliptical bell-mouth inlet was used with a square test section of 125 mm × 125 mm and of 335 mm in length, see Fig. 7. The cavity height is 493 mm and 119.25 mm in radius (internal dimensions). The orifice/opening between the cavity volume and the square test section of the wind tunnel has a wall thickness of 7.75 mm and a sharp chamfer at 45°—see Fig. 3. An array of 16 microphones was mounted in two rings of eight such that they were flush mounted with the inside of the cavity. Two 7 mm outside diameter G.R.A.S. microphones (model 40PR) and fourteen Sennheiser KE4 electret microphones were used. The Sennheiser microphones have a 20–20 000 Hz range and integrated pre-amplifiers and had been used successfully on previous projects. They were calibrated before the experimental campaign in an impedance tube with white noise produced by a B&K Noise Generator (type 1405) up to 20 kHz. The impedance tube has a radius of 25 mm: its cut-off frequency should be around 4 kHz. All the microphones were calibrated with respect to one of the two G.R.A.S. microphones for amplitude and phase. The electret microphones have an upper limit in amplitude of approximately 114 dB, however, before becoming nonlinear. It is for this reason that the G.R.A.S. microphones were employed so that they would be capable of analysing the much higher pressure amplitudes generated in the cylinder at high flow velocities. In the following analysis, the G.R.A.S. microphones are used for the measurements in plots such as in Figs. 10 and 14, etc., whereas the full set of 16 electret an G.R.A.S. microphones are used just for the modal decomposition at lower tunnel velocities. The two G.R.A.S. microphones were installed opposite each other (180° apart), with the location of the upstream one indicated by a black square in Fig. 1.

The 16 microphone configuration allows azimuthal modes of up to order $A_m = A_3$ to be resolved in both axial directions. A photograph of the rig is to be seen in Fig. 8. Each of the two rings of eight microphones were distributed equally in the circumferential direction. With regards to the axial spacing between the rings, s, this distance was chosen optimally so as to ensure that there were no drop-out frequencies in the frequency range of interest. A drop-out occurs at integer multiples of a frequency whose half wavelength is equal in length to the distance between the microphones, i.e., $f = c/(2s)$ and integer multiples thereof.

An error analysis performed by Åbom and Bodén,[43] provides a more comprehensive spacing guide which optimises s to minimise error at both low and high frequencies:

$$0.1\pi(1 - M^2) < \frac{2\pi f s}{c} < 0.8\pi(1 - M^2). \tag{6}$$

The two rings were therefore located at $x_1 = 125$ mm and $x_2 = 200$ mm as $s = 75$ mm ensures that no drop-outs occur in the frequency range of interest and that the lower limit is below the first longitudinal mode. The Helmholtz resonance, whilst excited below this lower limit, transpires to be of sufficiently high amplitude as to be measurable. The ×1 distance (and hence ×2) was chosen upon examination of the WEM analysis so as to ensure that the two rings of microphones were positioned so as not to align with acoustic nodes of the longitudinal standing waves in the frequency range of interest.

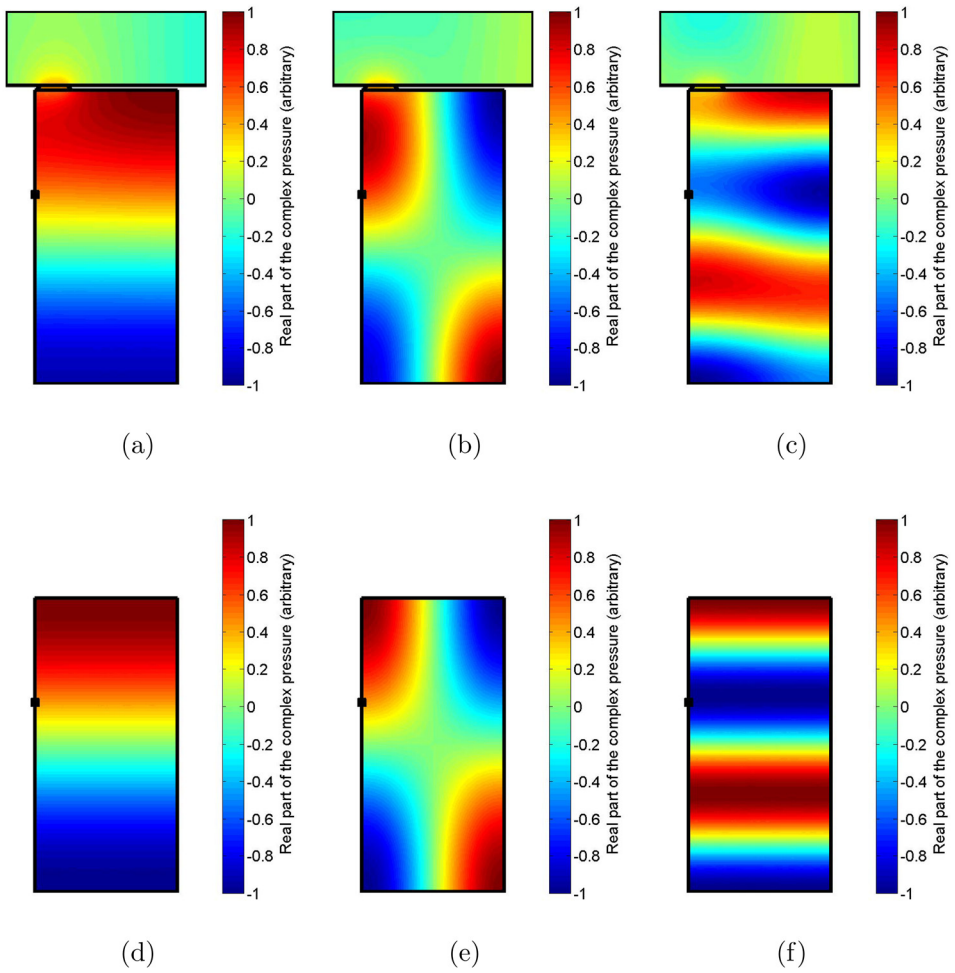

FIG. 6. (Color online) Normalized real pressure through the middle plane of the cavity. WEM results (first row) and analytical solutions (second row). Three modes are illustrated: (a) and (d) first longitudinal mode H1; (b) and (e) first azimuthal-longitudinal mode AZ1H1; (c) and (f) third longitudinal mode H3. The position of the pressure measurement point/microphone for the transfer function analysis is indicated by a black square.

IV. EXPERIMENTAL RESULTS

A. Preliminary results

Once the rig was built, some preliminary tests were performed to verify the cavity's response to excitation. Initially a opening of length $L = 45$ mm positioned upstream of the central axis of the cylinder ($\Delta = 184$ mm), similar to the set-up indicated in Fig. 1, was examined. This test point was called L45EU (edge upstream). An initial test was performed with a small loudspeaker radiating broadband noise located in the tunnel test section in the proximity of the orifice. A transfer function between the speaker input signal and one of the G.R.A.S. array microphones flush mounted with the inside surface of the cavity, indicated with a black square in Fig. 1, was calculated, and its magnitude is plotted in Fig. 9 (the center curve). Qualitatively, this compares extremely closely to a similar analysis performed on the numerical WEM data (the top curve), where the transfer function was calculated between the monopole source and a location equivalent to the microphone position. Each of the longitudinal, azimuthal, and combination modes are identified. The exception to this is the Helmholtz resonance in the numerical WEM data which poorly models the compressibility effect. In addition, there is a small (4 Hz) frequency shift between the WEM peaks and those measured with the speaker experiment. As the numerical solution has been found to be very sensitive to changes in the duct geometry, it is thought that this small discrepancy may be due to differences between the modelled and manufactured rig.

TABLE I. Frequencies, in Hz, of the acoustic modes of a cylindrical cavity ($D = 238$ mm and $H = 493$ mm) at 22 °C. Mode order (m, n, q): azimuthal, radial, longitudinal.

Mode	H1	H2	AZ1	AZ1H1	H3	AZ1H2	AZ1H3
(m, n, q)	(0,0,1)	(0,0,2)	(1,0,0)	(1,0,1)	(0,0,3)	(1,0,2)	(1,0,3)
He	0.8	1.54	1.84	2.02	2.30	2.42	2.95
Analytical	350	699	846	915	1049	1097	1347
WEM	365	706	842	930	1054	1111	1354

Similarly, the response from the same microphone located in the cavity is plotted for a tunnel flow velocity of approximately 21 m/s (the lower curve). Again there is excellent qualitative agreement with only very slight frequency difference between these results and those when using the loudspeaker. There is, however, a significant amount of low frequency noise which is presumed to originate from the centrifugal blower and ducting of the wind tunnel as well as hydrodynamic flow noise due to recirculating flow in the cavity which passes over the microphone sensor. In addition, as this flow speed does not result in a shear layer instability mode resonating with the Helmholtz resonance frequency, the Helmholtz peak does not appear in this curve. A full velocity sweep of the cavity in following tests allows this mode to be excited.

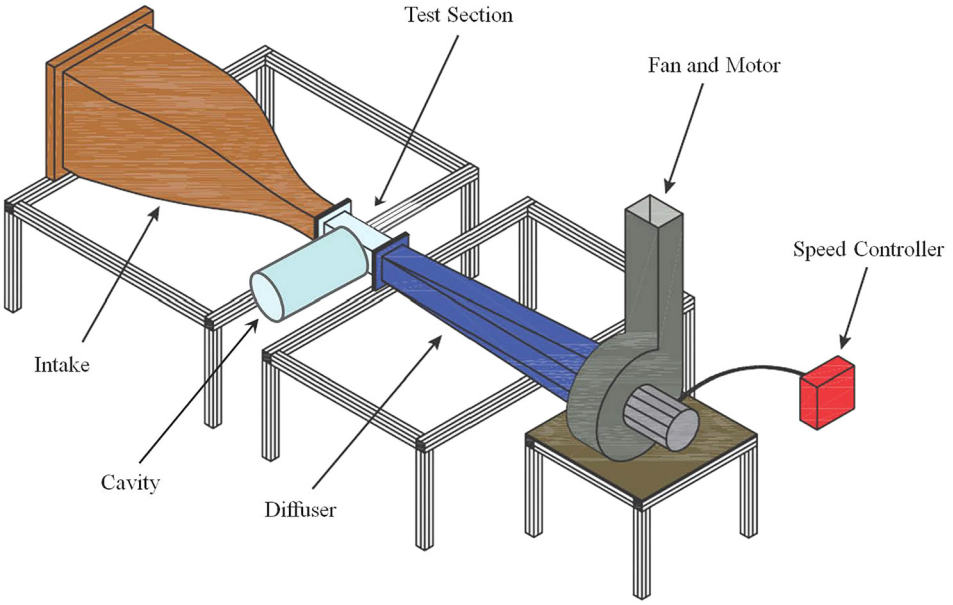

FIG. 7. (Color online) Schematic of the wind tunnel and cylindrical cavity.

Overall the various results agree very well with each other with the most significant deviation being between the three "real" sets of data, viz., WEM, speaker, and flow, which include the orifice, and the analytical model which does not. The disparities are most noticeable for H1 and AZ1H1 which have been noted to be most affected by the orifice, which causes an effective shortening of the cavity.

B. Baseline opening: Case L45EU

Following the initial tests, an automated velocity sweep of the tunnel was performed using LABVIEW to control the centrifugal blower motor speed controller. This approach allows the pressure field inside the cavity to be examined for the full range of flow speeds as per the objectives of the research. These results are presented in Fig. 10 with shear layer modes calculated according to Eq. (5) superimposed onto the plot. A range of convection speed coefficients are to be found in the literature.[2,11,32] A value of $\kappa = 0.42$ has been used here as a best fit to the measured data.

Audible tones in the region of the Helmholtz frequency were clearly heard and are seen in Fig. 10 to be excited at low flow speeds by the first shear layer instability mode (approximately 7 m/s). Given the thin wall forming the neck of the resonator, an "effective" neck length equal to the opening length ($l_s = L$) was used to calculate the Helmholtz resonance frequency as developed by Ma *et al.*,[11]

$$f_{HR} = \frac{c}{2\pi}\sqrt{\frac{S}{Vl_s}}, \tag{7}$$

where S is the plan-view cross sectional opening of the orifice, V is the volume of the cavity, c is the speed of sound, and l_s is the "effective" length of the slug of air that oscillates in the opening, or neck, of the cavity. For the geometry

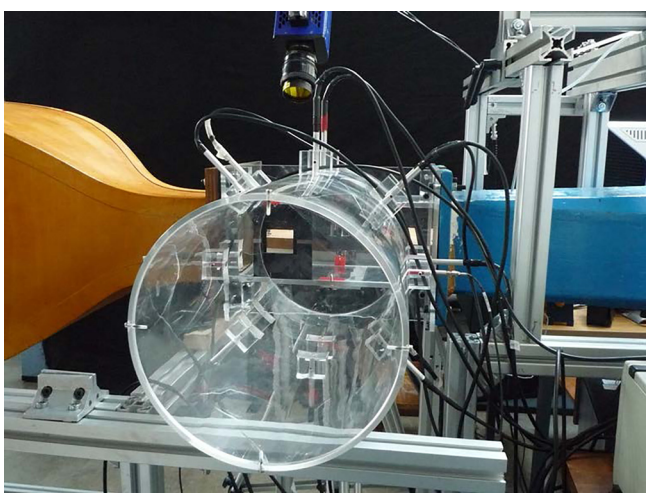

FIG. 8. (Color online) Photograph of cylindrical cavity and wind tunnel test section. To be seen is the orifice between the wind tunnel test section and the cavity as well as the 16 microphone array used for modal decomposition. Flow is from left to right.

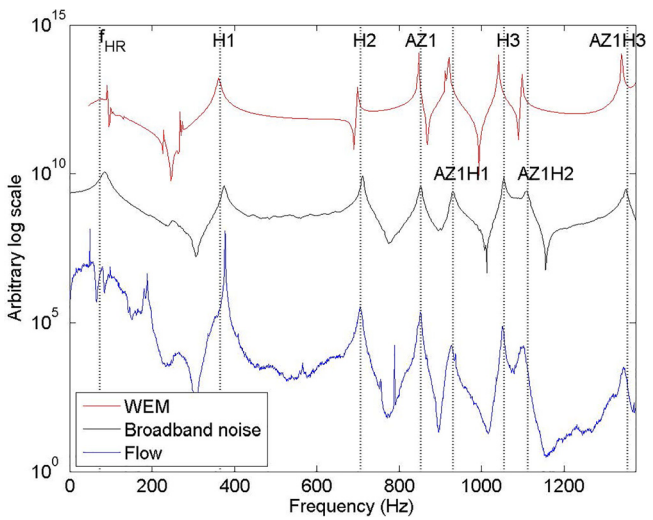

FIG. 9. (Color online) Response of the cavity to different excitations: monopole acoustic source (WEM: top curve), broadband loudspeaker noise (experimental: middle curve), and flow excited (experimental: bottom curve).

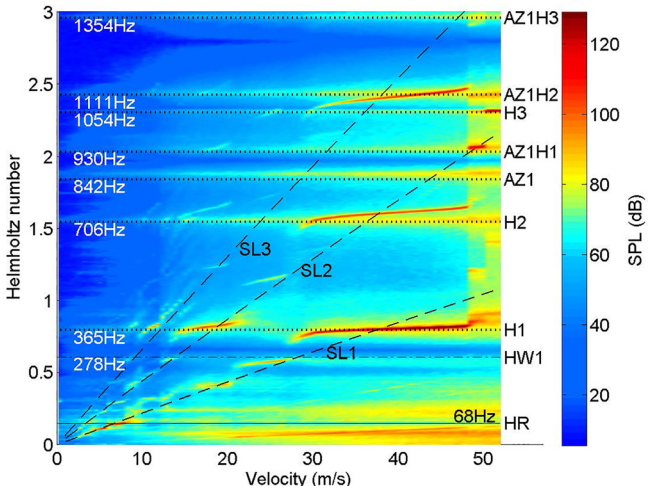

FIG. 10. (Color online) Acoustic response inside the cavity as a function of tunnel flow-speed. Superimposed on the plot are the theoretical shear layer modes (SL), the WEM acoustic modes (H1, AZ1,…) and the Helmholtz resonance (HR). The first longitudinal cavity/test section mode (HW1) calculated analytically is also reported. Frequencies are also given in non-dimensional form (Helmholtz number $= 2\pi fR/c$).

of this test-case, the theoretical value of 68 Hz superimposed on Fig. 10 compares extremely well with the measurements.

For higher flow speeds, an intense lock-in with the first cavity longitudinal mode (H1) is generated, again by the first shear layer instability mode. The amplitude of this tone is so great that a non-linear response is generated which results in the first and second harmonics to be excited and is seen in the plot at higher frequencies. As the H1 frequency for flow excitation (and WEM) are higher than the analytically predicted frequency, due to the effect of the opening, the harmonics do not align with the H2 and H3 frequencies, as expected, as these frequencies are less affected by the opening and are thus not integer multiples of H1. The lock-on subsequently drops out at higher velocities as the shear layer mode increases in frequency above the first longitudinal mode frequency. At higher velocities, the second shear layer mode locks onto first the AZ1H1 combination mode before subsequently locking onto the third longitudinal mode (H3). Lock-on switching back and forth between these frequencies was audible. A time/frequency domain analysis on this data has been performed to further examine this process.[44,45] The second and third shear layer modes also cause lock on with the H1 mode and amplification of the azimuthal and azimuthal combination modes (AZ1 and AZ1H1) is clearly evident at high velocities. Also identified in Fig. 10 is the combination longitudinal mode of wind tunnel width and cavity height (HW1). As the shear layer is bounded, transverse to the flow direction, by the wind tunnel wall on one side and by the cavity termination on the other, the first shear layer mode excites a standing wave which is formed between these two surfaces and can be seen to lock on at approximately 25 m/s.

C. Results from modal decomposition

In order to gain further insight into the modal content of the peaks seen in Fig. 10, a full azimuthal decomposition was performed in the cavity. A radial mode analysis was not performed on this set-up as radial modes cut-on above the frequency range of interest. For the modal array designed, the modal decomposition technique can solve for travelling waves in both the incident and reflected axial directions as well as for spinning azimuthal waves in both the clockwise and counterclockwise directions. As there is no mode rotation, the rotating modes are combined into one solution and the result is for the incident direction only (the reflected being effectively equal for this test set-up).

A modal decomposition of the acoustic field inside the cavity for a flow speed of 21 m/s using all sixteen of these microphones is given in Fig. 11. This is a very good result which shows clearly the modal content of the acoustic field in the cavity as a function of frequency, and agrees with the results given by the numerical WEM analysis from visualisation of the pressure patterns. Modes $A_m = A_2$ and $A_m = A_3$ have been included in the decomposition, but as they cut-on at higher frequencies (above He = 3) their modal amplitudes are calculated to be insignificant in this frequency range as expected. In accordance with theory, the H1 and H2 longitudinal modes are demonstrated from the modal decomposition to be plane waves, viz., $A_m = A_0$. Although the $A_m = A_1$ (AZ1) mode cuts-on at around He = 1.84, it does not remain dominant for all frequencies, with the plane wave mode $A_m = A_0$ constituting the H3 standing wave resonance. The value of the modal decomposition is seen upon examination of the combination modes AZ1H1, AZ1H2, and AZ1H3. Each of these contain a contribution of acoustic energy from the plane wave mode but it is the azimuthal component which dominates for each of these three modes.

As the equivalent numerical full-field pressure response information was available also from the WEM analysis, a modal decomposition was also performed on the pressure data output from the numerical solution. For each frequency at which the pressure field was calculated, a modal decomposition was performed using output from numerical mesh nodes corresponding to the microphone locations. The results for the WEM modal decomposition are given in Fig. 12. The result from this modal decomposition of the numerical data compares well with Fig. 11 with the main difference, as would be expected, being that the flow noise energy at low frequency is not present.

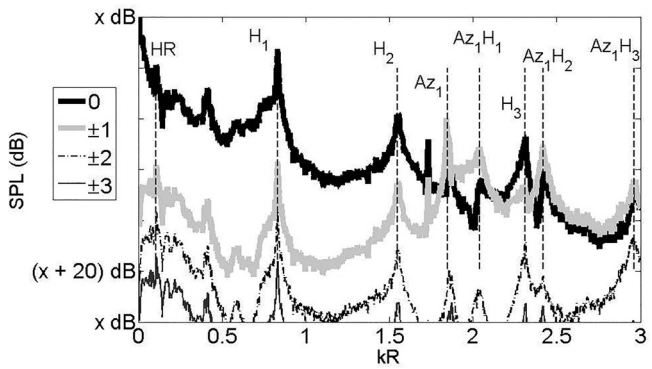

FIG. 11. Modal decomposition of the cylindrical cavity using experimental data. Tunnel velocity is 21 m/s.

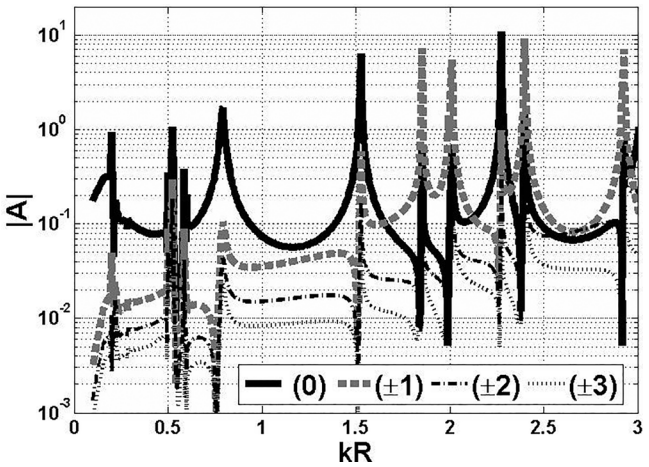

FIG. 12. Modal decomposition results using the WEM numerical data with pressure locations corresponding to the experimental microphone positions. Solution determined from response to monopole excitation as a function of frequency.

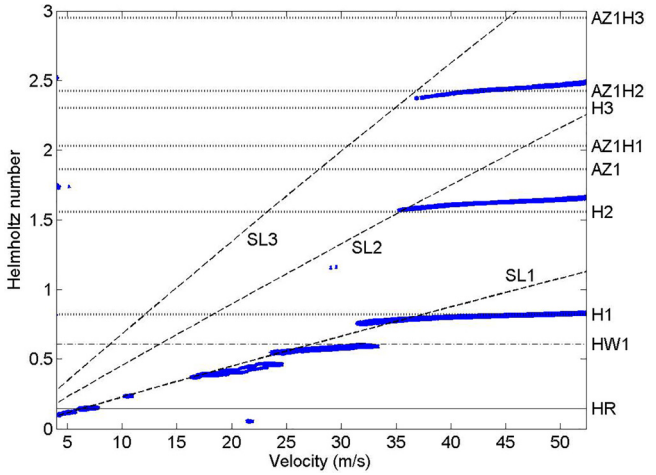

FIG. 14. (Color online) Contour of strength of lock-on higher than 13 dB. L40CC.

D. Influence of the location of the opening

The effect of the opening location was quantified. To improve the visibility of the pressure response in figures such as Fig. 10, the receptivity of the cavity to shear layer excitation was quantified using a "strength of lock-on (SoL)" parameter, as suggested by Mendelson[46] and described by Yang *et al.*[7] The parameter chosen was the amplification of the cavity pressure level above the background noise level. Three different positions were explored: $\Delta = 99$, 39, and 9 mm (L40CC, L40HD, and L40ED, respectively), refer to Fig. 13. CC, HD, and ED were used in the test matrix definition and indicated: centre/centre, halfway downstream, and edge downstream. The results are summarized in Figs. 14, 15, and 16, where the contour lines encircle values of SoL higher than 13 dB. The threshold criterion is a useful and straightforward technique to identify the resonance conditions in a flow excited cavity. The value of 13 dB was chosen by trial and error, and for this data, was found to capture all the significant resonance conditions while confining the contour levels to distinct regions that might otherwise blend together.

There are some very significant differences between the three openings analysed. It is clear that the resonance lock-on for H1 is much stronger when the opening is in the center of the cavity (L40CC): the first shear layer hydrodynamic mode remains locked-on with H1 for a wider range of velocities than for the other two orifice positions. Especially noteworthy is the cut-on of the azimuthal mode AZ1H1 at velocities above 45 m/s for L40ED and L40HD, which does not occur for L40CC. When the opening is off-center, the shear layer pressure fluctuations tend to excite AZ1H1 because they are closer to an acoustic anti-node. On the contrary, the central location is a pressure node for this acoustic mode as seen in Fig. 6(b). The third longitudinal mode is excited by the shear layer mode II from 50.3 to 52.3 m/s for L40HD while this resonance occurs only for the highest tested flow speed for L40ED.

It is very significant to note that the higher order modes AZ1 and AZ1H1 are both exited by shear layer excitation, refer to Fig. 9, a point almost unreported in the literature. However, for the 13 dB threshold set, whereas the azimuthal combination mode AZ1H1 tends to lock-on by the off-center orifice locations, the pure AZ1 azimuthal mode tends not to respond with such a high response. The vortex sound theory developed by Howe[47] is a good start in order to explain the predilection for certain specific eigenmodes for a flow-acoustic coupling. In Howe's acoustic analogy, the Coriolis density forces $\rho_0 \vec{w} \times \vec{u}$ are identified as the principal source of sound. The acoustic power generated by the vortical field Π can be calculated by equation

$$\Pi = -\rho_0 \int_V (\vec{w} \times \vec{v}) \cdot \vec{u}_{acoust} \, dV, \tag{8}$$

which states that the Π is proportional to the triple product $\vec{u}_{acoust} \cdot (\vec{w} \times \vec{u})$ between the vorticity, $\vec{w}$, the hydrodynamic velocity, $\vec{v}$, and the acoustic particle velocity, $\vec{u}_{acoust}$, in the volumetric flow field V with mean density ρ_0. From this formula, it is clear that if the acoustic particle velocity at the opening has the same orientation as the velocity or the vorticity, there is no acoustic power generated. Let us now take the example of the first azimuthal mode (AZ1). It has been shown numerically, Fig. 5, that this mode is symmetrical about the plane perpendicular to the flow (it could have been symmetrical about any other vertical plane; however, the

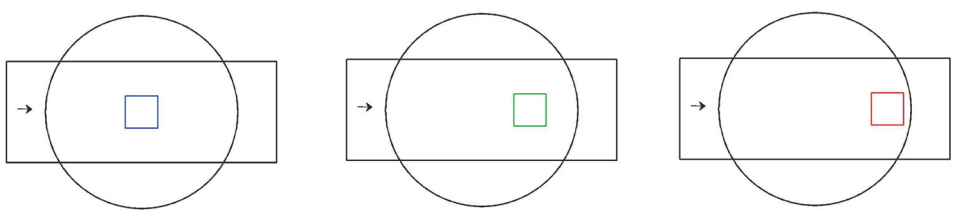

FIG. 13. (Color online) Orifice locations: L40CC, L40HD, and L40ED.

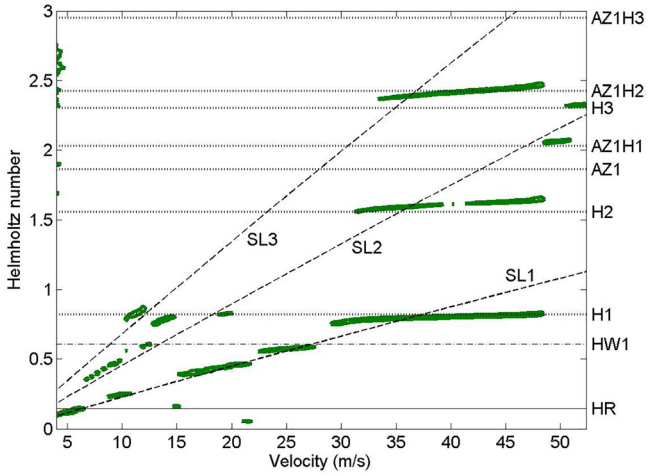

FIG. 15. (Color online) Contour of strength of lock-on higher than 13 dB. L40HD.

opening location imposes the symmetry plane). The mode AZ1 does not radiate sound because the acoustic particle velocity has the same orientation as the mean flow. This is a very simplistic explanation especially because it assumes the directions of $\vec{u}_{acoust}$, $\vec{w}$, and $\vec{u}$ to be known *a priori*.

V. CONCLUSIONS

A cylindrical cavity experiment which allows different modes of resonant behaviour to be excited depending on flow speed and orifice geometry has been designed and constructed. Specifically, modes falling into the fluid-resonant category, viz., Helmholtz resonance, longitudinal resonance, and azimuthal resonance, have all been excited by different shear layer oscillation modes. Lock-on between these different resonant modes and shear layer excitation has been clearly measured and observed to occur upon adjusting only the flow speed. The effect of the cavity opening location on the internal resonance was also studied, and found to be a major factor in determining which modes were excited. Specifically, azimuthal modes were only found when the excitation was not located at the center of the cavity, which would be a node for the azimuthal mode. A modal decomposition technique was performed on both the experimental and numerical data and provided diagnostic insight into the modal content of each of the resonant modes.

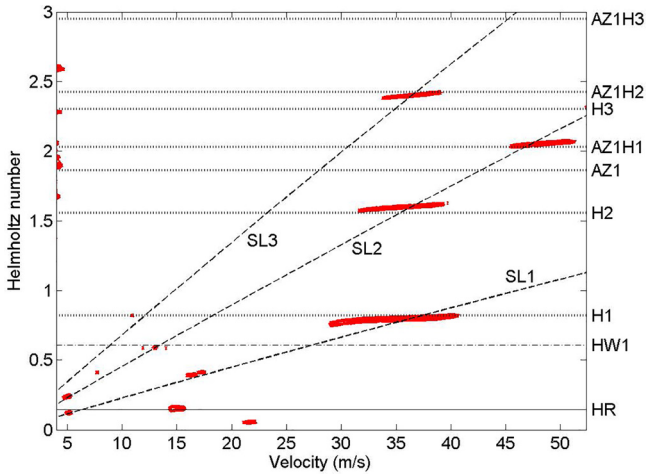

FIG. 16. (Color online) Contour of strength of lock-on higher than 13 dB. L40ED.

ACKNOWLEDGMENTS

D.B.S. was supported as a visiting scholar to Trinity College Dublin by the Erasmus Mundus Master of Mechanical Engineering programme before taking up his position in NASA. F.R.V. spent this research period in Trinity College Dublin as a graduate student and was supported by a Marie Curie Early Stage Research Training grant. The research leading to these results has received funding from the European Union's Seventh Framework Programme (Grant No. FP7/2007-2013) for the Clean Sky Joint Technology Initiative under grant agreement No. 620188.

[1]D. Rockwell and E. Naudascher, "Review—Self-sustained oscillations of flow past cavities," J. Fluids Eng. **100**, 152–165 (1978).
[2]J. E. Rossiter, "Wind-tunnel experiments on the flow over rectangular cavities at subsonic and transonic speeds," Technical Report No. R&M 3438, Aeronautical Research Council (1964).
[3]R. B. Langtry and P. R. Spalart, "DES investigation of a baffle device for reducing landing-gear cavity noise," in *46th AIAA Aerospace Sciences Meeting and Exhibit*, Reno, NV, USA (January 7–10, 2008).
[4]G. Balasubramanian, B. Crouse, and D. Freed, "Numerical simulation of leakage effects on sunroof buffeting of an idealized generic vehicle," in *15th AIAA/CEAS Aeroacoustics Conference*, Miami, FL, USA (May 11–13, 2009).
[5]Denis Ricot, Virginie Maillard, and Christophe Bailly, "Numerical simulation of the unsteady flow past a cavity and application to the sunroof buffeting," in *7th AIAA/CEAS Aeroacoustics Conference and Exhibit*, Aeroacoustics Conferences, American Institute of Aeronautics and Astronautics (2001).
[6]D. Tonon, A. Hirschberg, J. Golliard, and S. Ziada, "Aeroacoustics of pipe systems with closed branches," Int. J. Aeroacoust. **10**, 201–276 (2011).
[7]Y. Yang, D. Rockwell, K. Lai-Fook Cody, and M. Pollack, "Generation of tones due to flow past a deep cavity: Effect of streamwise length," J. Fluids Struct. **25**, 364–388 (2009).
[8]P. Oshkai and T. Yan, "Experimental investigation of coaxial side branch resonators," J. Fluids Struct. **24**, 589–603 (2008).
[9]R. L. Panton and J. M. Miller, "Resonant frequencies of cylindrical Helmholtz resonators," J. Acoust. Soc. Am. **57**(6), 1533–1535 (1975).
[10]H. Kook and L. Mongeau, "Analysis of the periodic pressure fluctuations induced by flow over a cavity," J. Sound Vib. **251**, 823–846 (2002).
[11]R. Ma, P. E. Slaboch, and S. C. Morris, "Fluid mechanics of the flow-excited Helmholtz resonator," J. Fluid Mech. **623**, 1–26 (2009).
[12]S. A. Elder, "Self-excited depth-mode resonance for a wall-mounted cavity in turbulent flow," J. Acoust. Soc. Am. **64**, 877–890 (1978).
[13]K. Awny and S. Ziada, "Effect of cavity depth on diametral mode excitation," in *9th International Conference on Flow-Induced Vibrations (FIV2008)*, Prague, Czech Republic (2008).
[14]P. Oshkai, M. Geveci, D. Rockwell, and M. Pollack, "Imaging of acoustically coupled oscillations due to flow past a shallow cavity: Effect of cavity length scale," J. Fluids Struct. **20**, 277–308 (2005).
[15]J. Hsu and K. Ahuja, "Cavity noise control using Helmholtz resonators," Paper No. AIAA-96-1675 (1996).
[16]L. Cattafesta, D. Williams, C. Rowley, and F. Alvi, "Review of active control of flow-induced cavity resonance," AIAA Paper No. 3567 (2003), p. 2003.
[17]C. W. Rowley and D. R. Williams, "Dynamics and control of high-Reynolds-number flow over open cavities," Annu. Rev. Fluid Mech. **38**, 251–276 (2006).
[18]O. Marsden, C. Bailly, C. Bogey, and E. Jondeau, "Investigation of flow features and acoustic radiation of a round cavity," J. Sound Vib. **331**, 3521–3543 (2012).

[19]J. Kennedy, E. Neri, and G. J. Bennett, "The reduction of main landing gear noise (AIAA 2016-2900)," in *22nd AIAA/CEAS Aeroacoustics Conference*, Lyon, France (2016).
[20]Eleonora Neri, John Kennedy, and Gareth J. Bennett, "Aeroacoustic source separation on a full scale nose landing gear featuring combinations of low noise technologies," in *Internoise2015: Proceedings of the Internoise 2015/ASME NCAD Meeting*, American Society of Mechanical Engineers, San Francisco, CA, USA (2015).
[21]Eleonora Neri, John Kennedy, Massimiliano Di Giulio, Ciaran O'Reilly, Jeremy Dahan, Marco Esposito, Massimiliano Bruno, Francesco Amoroso, Antonello Bianco, and Gareth J. Bennett, "Characterization of low noise technologies applied to a full scale fuselage mounted nose landing gear," in *Internoise2015: Proceedings of the Internoise 2015/ASME NCAD Meeting*, Paper No. IN2015-350, American Society of Mechanical Engineers, San Francisco, CA, USA (2015).
[22]Eleonora Neri, John Kennedy, and Gareth J. Bennett, "Noise characterization and noise treatment of a detailed full scale nose landing gear," in *Greener Aviation: Achievements and Perspectives in Clean Sky and Worldwide, Brussels, Belgium*, 3AF—Association Aéronautique et Astronautique de France, Brussels, Belgium (October, 2016).
[23]John Kennedy, Eleonora Neri, and Gareth J. Bennett, "An experimental investigation of the contributions of cavity resonance and vortex shedding to the noise emission of main landing gear," in *Greener Aviation: Achievements and Perspectives in Clean Sky and Worldwide, Brussels, Belgium*, 3AF—Association Aéronautique et Astronautique de France, Brussels, Belgium (October, 2016).
[24]Saloua Ben Khelil, "ZDES simulation of the noise emission of a regional aircraft main landing gear bay with opened or closed doors," in *Greener Aviation: Achievements and Perspectives in Clean Sky and Worldwide, Brussels, Belgium*, 3AF—Association Aéronautique et Astronautique de France, Brussels, Belgium (October, 2016).
[25]Ian Davis and Gareth J. Bennett, "Novel noise-source-identification technique combining acoustic modal analysis and a coherence-based noise-source-identification method," AIAA J. **53**, 3088–3101 (2015).
[26]M. Åbom, "Modal decomposition in ducts based on transfer function measurements between microphone pairs," J. Sound Vib. **135**, 95–114 (1989).
[27]P. Yardley, "Measurement of noise and turbulence generated by rotating machinery," Ph.D. thesis, University of Southampton, Southamton, UK (1974).
[28]M. Åbom, "Modal decomposition in ducts based on transfer function measurements between microphone pairs," Technical Report No. TRITA-TAK-8702, Department of Technical Acoustics, Royal Institute of Technology, Stockholm, Sweden (1987).
[29]F. Castres and P. Joseph, "Mode detection in turbofan inlets from near field sensor arrays," J. Acoust. Soc. Am. **121**, 796–807 (2007).
[30]F. Holste and W. Neise, "Noise source identification in a propfan model by means of acoustical near field measurements," J. Sound Vib. **203**, 641–665 (1997).
[31]G. Bennett, "Noise source identification for ducted fans," Ph.D. thesis, Trinity College Dublin, Dublin, Ireland (2006).
[32]F. Rodriguez Verdugo, A. Guitton, R. Camussi, and M. Grottadaurea, "Experimental investigation of a cylindrical cavity," in *15th AIAA/CEAS Aeroacoustics Conference*, Miami, FL (2009), pp. 2009–3207.
[33]L. Chatellier, J. Laumonier, and Y. Gervais, "Theoretical and experimental investigations of low Mach number turbulent cavity flows," Exp. Fluids **36**, 728–740 (2004).
[34]M. El Hassan, L. Labraga, and L. Keirsbulck, "Aero-acoustic oscillations inside large deep cavities," in *16th Australasian Fluid Mechanics Conference*, Australia (2007).
[35]H. H. Heller and D. B. Bliss, "The physical mechanism of flow induced pressure fluctuations in cavities and concepts for suppression," in *2nd AIAA Aeroacoustics Conference*, Hampton, VA (1975), pp. 75–491.
[36]M. S. Howe, "Edge, cavity and aperture tones at very low Mach numbers," J. Fluid Mech. **330**, 61–84 (1997).
[37]J. E. Caruthers, R. C. Engels, and G. K. Ravinprakash, "A wave expansion computational method for discrete frequency acoustics within inhomogeneous flows," in *2nd AIAA/CEAS Aeroacoustic Conference*, State College, PA (1996).
[38]G. Ruiz and H. J. Rice, "An implementation of a wave-based finite difference scheme for a 3-d acoustic problem," J. Sound Vib. **256**, 373–381 (2002).
[39]L. B. Rolla and H. Rice, "A forward-advancing wave expansion method for numerical solution of large-scale sound propagation problems," J. Sound Vib. **296**, 406–415 (2006).
[40]G. J. Bennett, C. J. O'Reilly, and H. Liu, "Modelling multi-modal sound transmission from point sources in ducts with flow using a wave-based method," in *16th Congress on Sound and Vibration*, Krakow, Poland (2009).
[41]F. R. Verdugo, R. Camussi, and G. J. Bennett, "Aeroacoustic source characterization technique applied to a cylindrical helmholtz resonator," in *The 18th International Congress on Sound and Vibration (ICSV18)*, Paper No. 2062, Rio de Janeiro, Brazil (2011).
[42]G. J. Bennett, F. R. Verdugo, and D. B. Stephens, "Shear layer dynamics of a cylindrical cavity for different acoustic resonance modes," in *15th International Symposium on Applications of Laser Techniques to Fluid Mechanics*, Paper No. 1727, Lisbon, Portugal (2010).
[43]M. Åbom and H. Bodén, "Error analysis of two-microphone measurements in ducts with flow," J. Acoust. Soc. Am. **83**, 2429–2438 (1988).
[44]D. B. Stephens, F. Rodriguez Verdugo, and G. J. Bennett, "Shear layer driven acoustic modes in a cylindrical cavity (AIAA 2010-3903)," in *16th AIAA/CEAS Aeroacoustics Conference*, Stockholm, Sweden (2010).
[45]D. B. Stephens, F. R. Verdugo, and G. J. Bennett, "Shear layer driven acoustic modes in a cylindrical cavity," J. Pressure Vessel Technol. (ASME) **136**(5), 051309 (2014).
[46]R. S. Mendelson, "Methods of measuring lock-in strength and their application to the case of flow over a cavity locking into a single sidebranch," in *9th AIAA/CEAS Aeroacoustics Conference*, Hilton Head, SC, USA (2003), pp. 2003–3106.
[47]M. S. Howe, "Contributions to theory of aerodynamic sound, with application to excess jet noise and the theory of the flute," J. Fluid Mech. **71**(4), 625–673 (1975).